Carbon isotopes of Proterozoic filamentous microfossils: SIMS analyses of ancient cyanobacteria from two disparate shallow-marine cherts

Jeffrey T. Osterhout, J. William Schopf, Kenneth H. Williford, Kevin D. McKeegan, Anatoliy B. Kudryavtsev & Ming-Chang Liu

View supplementary material

Published online: 01 Jul 2021.

Submit your article to this journal

Article views: 72

View related articles

View Crossmark data

Taylor & Francis
Taylor & Francis Group

Check for updates

Carbon isotopes of Proterozoic filamentous microfossils: SIMS analyses of ancient cyanobacteria from two disparate shallow-marine cherts

Jeffrey T. Osterhout[a,b] (ID), J. William Schopf[a,b], Kenneth H. Williford[c], Kevin D. McKeegan[a], Anatoliy B. Kudryavtsev[a,b], and Ming-Chang Liu[a]

[a]Department of Earth, Planetary, and Space Sciences, University of California, Los Angeles, CA, USA; [b]Center for the Study of Evolution and the Origin of Life, University of California, Los Angeles, CA, USA; [c]Jet Propulsion Laboratory, California Institute of Technology, Pasadena, CA, USA

ABSTRACT

The surface ecosystem of the Precambrian Earth was dominated by marine, planktonic and benthic phototrophic microorganisms, most prominently stromatolite-forming cyanobacteria, anoxygenic photosynthetic bacteria, and associated microbes. Although coupling the early microfossil record to physiologically definitive geochemical and isotopic signatures remains challenging, insights can be derived from isotopic studies of individual fossil microorganisms permineralized in Precambrian cherts. Here, we use correlated optical microscopy, Raman spectroscopy, and secondary ion mass spectrometry (SIMS) to link morphology with the molecular and carbon isotopic composition ($\delta^{13}C_{org}$) of individual filamentous microfossils (*Eomycetopsis* sp.) composed of thermally immature kerogen and preserved in two spatially and temporally distinct shallow-marine cherts of the Proterozoic Gaoyuzhuang Formation (~1,560 Ma, northern China) and Kwagunt Formation (~850 Ma, Arizona, USA). In both geologic units studied, the *Eomycetopsis* fossils yielded virtually indistinguishable $\delta^{13}C_{org}$ values (−29.0 ± 2.0‰) that are comparable to values resulting from carbon fixation via the RuBisCO enzyme in the Calvin cycle of oscillatoriacean cyanobacteria, the main oxygenic phototrophs of the Proterozoic.

Introduction

Prior to the ~541 Ma 'Cambrian explosion of animal life,' microorganisms inhabiting aquatic environments prevailed throughout Earth's biosphere. Such Precambrian, mostly prokaryotic microbes, contain carbonaceous cell walls commonly well-preserved by permineralization (i.e. 'petrifaction') and exhibit relatively simple morphologies, including spheroids – both solitary and aggregated in sheath-enclosed colonies – and unbranched multi-celled filaments along with their vacated enclosing cylindrical sheaths (e.g. Javaux and Lepot 2018; Schopf 1968, 1992; Schopf et al. 2007). Paleobiological interpretations of such taxa have traditionally been based on detailed morphological comparison with similar extant microorganisms, their metabolism inferred from these comparisons and their environmental setting (Knoll 1985b, 2012; Schopf 1968; Schopf et al. 2015). Relatively recent developments in ion microprobe analyses of individual carbonaceous microfossils (e.g. House et al. 2000; Oehler et al. 2017; Ueno et al. 2001; Williford et al. 2013) permit in situ comparisons of morphological, geochemical, and carbon isotopic data to more definitively guide interpretations of ancient Precambrian ecosystems.

Many formally described Precambrian microfossils have been classified as cyanobacteria, oxygen-producing photosynthesizers, evidently extant millions of years into the Archean and well preceding the ~2.2–2.4 Ga Great Oxidation Event (GOE) (e.g. Anbar et al. 2007; Awramik 1992; Bosak et al. 2009; Buick 1992, 2008; Kaufman et al. 2007). Some such taxa exhibit distinctively diagnostic cyanobacterial characteristics, which can be compared in cell-by-cell detail with genera and even species of extant Oscillatoriaceans, Nostocaceans, and Chroococcaceans (Hofmann 1976; Schopf 1968), whereas others, particularly those reported from Archean deposits, are less informative (e.g. Awramik et al. 1983; Klein et al. 1987; Ueno et al. 2001; Walsh and Lowe 1985). While oscillatoriacean cyanobacteria represent the most commonly reported group of photosynthetic prokaryotes in the fossil record, their diversity and evolutionary origin prior to the GOE remains uncertain (Butterfield 2015; Golubic and Seong-Joo 1999; Schopf 2011; Sergeev et al. 2012). This seeming disparity between the Proterozoic and Archean fossil records is not surprising. Sediments surviving to the present from the Proterozoic are vastly more abundant than those of the older Archean and, with but few exceptions, are decidedly less geologically and geochemically altered. Thus, the more

voluminous and better preserved Proterozoic fossil record is considered to be a useful reference for interpretation of putative Archean microfossil-like structures (Knoll 1985a; Schopf et al. 2007).

In the Proterozoic – as in modern microbial mat communities – photoautotrophic cyanobacteria were primary contributors to the formation of such shallow-marine sedimentary structures as stromatolites (e.g. Grotzinger and Knoll 1999), and their role in localized mineral precipitation has been implicated as well in the generation of pisolites, oncolites (e.g. Knoll et al. 1989; Swett and Knoll 1989), and cherty and carbonate chemical sediments (e.g. Kremer et al. 2012). Diverse types of cyanobacteria have also been recorded actively photosynthesizing within extant stromatolitic microbial mat communities (e.g. Burns et al. 2004; Reid et al. 2000).

The geochemical composition of individual Precambrian microfossils has recently been used both to verify and revise initial taxonomic classifications, and secondary ion mass spectrometry (SIMS) analyses of their stable carbon isotope ($\delta^{13}C$) compositions have revealed differences among Proterozoic and Archean microbial assemblages (e.g. House et al. 2000, 2013; Schopf et al. 2018), and between morphologically distinct microfossils (Williford et al. 2013) that previously had been masked in bulk (~25 g) analyses of whole-rock samples (see Strauss et al. 1992a, 1992b; Strauss and Moore 1992). These bulk mixtures are necessarily dominated by the prime organic carbon source, which consists of particulate detrital kerogen in addition to the preserved microbiota.

In the Precambrian, secular changes in the global carbon cycle are controlled by long-term variations in the fractional burial of organic carbon, most being recycled into the biosphere (Hayes et al. 1999; Des Marais 2001). Nevertheless, the $25 \pm 10‰$ offset between $\delta^{13}C_{org}$ and $\delta^{13}C_{carb}$ has remained essentially constant throughout most of geologic history (Hayes et al. 1983, 1999; Schidlowski 2001). This robust isotopic difference between organic and inorganic carbon in Precambrian sedimentary rocks is primarily due to the preferential uptake of ^{12}C relative to ^{13}C during biological carbon fixation by primary producers. In photoautotrophs such as cyanobacteria (and higher plants), the ribulose-1,5-bisphosphate carboxylase/oxygenase (RuBisCO) enzyme is the biological molecule primarily responsible for the kinetic isotope effect that discriminates between ^{12}C and ^{13}C (e.g. Farquhar et al. 1989; Hayes 1993). Thus, organic biomass becomes ^{13}C-depleted relative to the ^{13}C-enriched inorganic carbon (atmospheric CO_2 and its dissolved carbonate rock-generating derivative, HCO_3^-), both signatures frequently preserved within minimally altered sedimentary rock units (Hayes et al. 1999; Schidlowski 2001).

Despite the great inroads in deciphering the Precambrian fossil record since the inception of the modern field in the mid-1960s, it has been difficult to reliably assess the physiological similarities (or differences) of morphologically comparable microfossils separated both spatially and temporally in the rock record. The fossils of the ~1,560 Ma Gaoyuzhuang Formation of Jixian, China and the ~850 Ma

Kwagunt Formation of Arizona, U.S.A., meet this need – the deposits are geographically and temporally distinct, both contain microbial assemblages preserved by permineralization in shallow marine cherts, and many of their biotic components are morphologically virtually identical.

Studied samples of the Gaoyuzhuang Formation microbiota are preserved in finely laminated stromatolites, indicative of a relatively quiescent setting, whereas the fossiliferous Kwagunt cherts are pisolitic, deposited in a more agitated shallow-marine environment. In both deposits filamentous microfossils are abundant, widespread and three-dimensionally preserved. In the petrographic thin sections studied, small portions and occasionally longer parts of whole filaments are exposed at thin section surfaces, in most instances free from background detrital kerogen making them particularly suitable for in situ SIMS carbon isotope analyses. SIMS measurements of individual fossil filaments in the two deposits thus provides a current state-of-the-art method to assess the physiological similarities (or differences) of comparably preserved, morphologically similar microfossils, widely separated both in space and time.

Materials and methods

Geologic units studied

The Mesoproterozoic ~1,560 Ma Gaoyuzhuang Formation (Jixian Group of northern China) is a shallow-marine subtidal deposit containing abundant silicified conical stromatolites. Permineralized within the stromatolitic chert layers are unbranched, cylindrical, 2–4 μm-broad filamentous microfossils referred to Eomycetopsis sp. and interpreted to represent extracellular originally mucilaginous sheaths of oscillatoriacean cyanobacteria preserved as a result of early diagenetic silicification (Schopf et al. 1984; Zhang 1981). In addition, here analyzed from the Gaoyuzhuang cherts are larger-diameter (30–40 μm-wide) tubules similar to the originally trichome-encompassing sheaths of Lyngbya-like oscillatoriaceans (e.g. Schopf et al. 1984; Schopf and Sovietov 1976).

Carbonate rocks of the Gaoyuzhuang Formation evidence physically stable marine conditions and have carbon isotope ($\delta^{13}C_{carb}$) values that average $-0.5 \pm 0.5‰$ and range from approximately $-3‰$ to $+1‰$ (Chu et al. 2004, 2007; Guo et al. 2013; Hongwei et al. 2011). Of numerous carbonates analyzed from the five formations of the Jixian Group (Guo et al. 2013) – in total having an average $\delta^{13}C_{carb}$ of $-0.3‰$ and ranging between $-1‰$ and $+1‰$ (with the exception of a 50-m interval that records a negative excursion to $-2.5‰$) – those of the Gaoyuzhuang Formation exhibit the least $\delta^{13}C_{carb}$ variability.

Bulk (25-g sample) $\delta^{13}C_{org}$ values for carbonaceous matter in Gaoyuzhuang chert and carbonate lithologies range from $-32.0‰$ to $-26.4‰$, and average $-30.9‰$ for total organic carbon ($n = 8$) and $-31.2‰$ for extracted kerogens ($n = 2$) (Strauss et al. 1992b; Strauss and Moore 1992), values a few per mil lower than the average of $-27.4 \pm 1.2‰$ for total organic carbon ($n = 5$) earlier reported by Schopf et al. (1984).
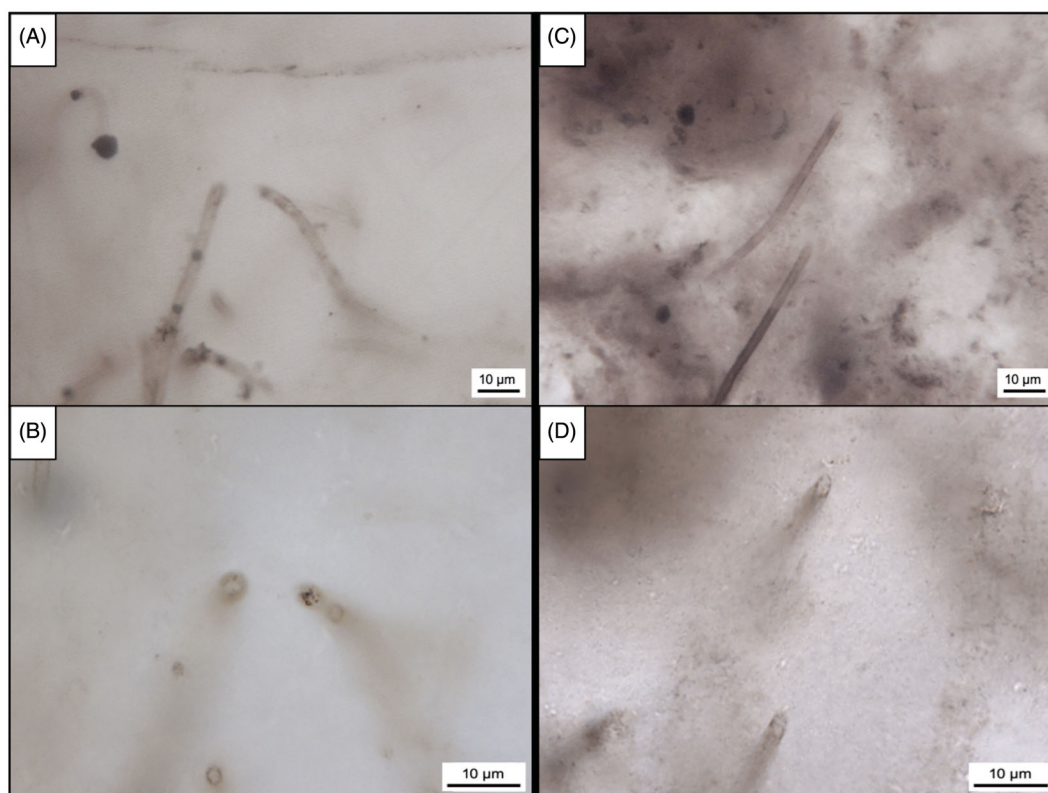
Figure 1. Transmitted light photomicrographs of permineralized kerogenous microfossil filaments (*Eomycetopsis* sp.) in petrographic thin sections of cherts from the Kwagunt Formation (A, B) and Gaoyuzhuang Formation (C, D). The photomicrographs in B and D illustrate the three-dimensional preservation of the fossils exposed at thin section surfaces, whereas the composite photomontages of stacked images (A, C) illustrate the filamentous morphology of multiple microfossils within the field of view.

The minimum age of the Gaoyuzhuang Formation is constrained by U-Pb determinations of $1,559 \pm 12$ Ma measured by SIMS (SHRIMP) and $1,560 \pm 5$ Ma (LA-MC-ICPMS) in zircons from a tuff bed in the upper Gaoyuzhuang Formation (Li et al. 2010), refined from an earlier reported Pb-Pb age of $1,435 \pm 50$ Ma (Schopf et al. 1984) and assumed age of $\sim 1,425$ Ma (e.g. Moore and Schopf 1992). Additional U-Pb age data from volcanics of the underlying Dahongyu Formation provide a maximum age of $1,625 \pm 6.2$ Ma (Lu and Li 1991; Meng et al. 2011) for the fossiliferous cherts studied here.

The other geological unit here investigated, the Neoproterozoic Kwagunt Formation of the upper Chuar Supergroup in the Grand Canyon, Arizona (U.S.A.) is a shallow-marine peritidal deposit, the pisolitic cherts of the Walcott Member containing permineralized filamentous microfossils. The fossiliferous pisolites formed in a mildly agitated, tidally influenced setting through the sequential accretion of thin siliceous rinds that were repeatedly colonized by microbial communities (Schopf et al. 1973). The 2–4 μm-broad filamentous 'Eomycetopsis-like' Kwagunt microfossils reported by Schopf et al. (1973) are morphologically closely similar to the *Eomycetopsis* specimens analyzed from the Gaoyuzhuang cherts (Figure 1).

Most of the $\delta^{13}C_{carb}$ values measured for carbonates from the Walcott Member of the upper Kwagunt Formation fall within a wide range extending from -6% to $+5\%$, with an average of $-1.1 \pm 3.5\%$; however, the least geochemically

altered samples have values close to zero (Karlstrom et al. 2000; Summons et al. 1988). Bulk (~ 25 g) $\delta^{13}C_{org}$ values for carbonaceous matter extracted from shales, carbonates and cherts of the Kwagunt Formation range from -27.7% to -26.1% and average approximately -26.7% ($n = 8$) (Strauss and Moore 1992), a value similar to earlier reported $\delta^{13}C_{org}$ values of $-25.7 \pm 0.13\%$ ($n = 4$) for bulk kerogens and acid-macerated *Melanocyrillium* vase-shaped microfossils extracted from Kwagunt shales (Bloeser 1985). Notably, all of these values fall within the broader range of -28% to -22% (average $= -25.6 \pm 1.3\%$) measured throughout the Chuar Group strata (Karlstrom et al. 2000) and are similar to the average $\delta^{13}C_{org}$ value of -25.9% of carbonaceous matter analyzed in two additional Chuar Group carbonates (Summons et al. 1988).

The age of the Kwagunt Formation is estimated for the Walcott Member to be ~ 850 Ma (~ 830 to $\sim 1,090$ Ma) (Ford and Breed 1973; Moore and Schopf 1992) and is also constrained by a U-Pb age of 742 ± 6 Ma from an ash bed at the top of the Walcott Member (Karlstrom et al. 2000).

Bulk analyses of the $\delta^{13}C_{carb}$ and $\delta^{13}C_{org}$ compositions of the fossiliferous Gaoyuzhuang and Kwagunt Formations provide important reference points for evaluation of the SIMS analyses of individual microscopic fossils reported here from the two units. The $\delta^{13}C_{carb}$ and $\delta^{13}C_{org}$ values of the Gaoyuzhuang and Kwagunt Formations are similar (average $\delta^{13}C_{carb}$ values of $-0.5 \pm 0.5\%$ and $-1.1 \pm 3.5\%$, and average $\delta^{13}C_{org}$ values of -30.9% and -26.7%,

respectively), and they are typical of most other marine carbonate-dominated deposits analyzed from the Proterozoic rock record (Schidlowski 2001).

Sample preparation

Polished ∼50–150 µm-thick petrographic thin sections of cherts from the Gaoyuzhuang and Kwagunt Formations were surveyed using transmitted light optical microscopy to locate surface-exposed microfossils and associated detrital kerogen appropriate for SIMS analysis. Fossiliferous areas of thin sections containing surface-exposed filaments were cut into ∼1' round mounts suitable for the SIMS sample holder, the fossils being positioned as close to the center of the mount as possible to avoid unwanted effects from measurements near the sample edge. The samples and epoxy-mounted standards were cleaned and sonicated in deionized (DI) water three times for 1 min., rinsed in DI water after each treatment and then sonicated in ethanol for 30 s and again rinsed in DI water and sonicated for 1 min. The cleaned samples were then dried overnight in a vacuum oven at 50 °C. After cleaning, the target microfossils and associated kerogenous detritus in each mount were photographed using transmitted and reflected light at multiple magnifications (Figure 1) using a Leica DM6000 housed at the NASA Jet Propulsion Laboratory (JPL) Astrobiogeochemistry Laboratory (abcLab), and their stage coordinates were documented relative to diamond scribe-inserted fiducial marks near the section edges.

Scanning electron microscopy (SEM) of the analyzed specimens was then performed at the JPL abcLab using a Hitachi SU-3500 SEM to acquire images in secondary and backscattered electron modes. After applying a 3-nm-thick platinum (Pt) veneer to the sample surface, SEM images were acquired under high vacuum using an accelerating voltage of 15 keV at a working distance of ∼7 mm.

Prior to subsequent SIMS analyses at UCLA's W.M. Keck Foundation Center for Isotope Geochemistry, the mounts were covered with a thicker (∼30 nm) gold coat required for conductivity, and were degassed overnight in the SIMS sample storage chamber. After each SIMS analysis session, the gold coat was removed with a 0.1-µm aluminum oxide polishing solution, and each specimen was re-imaged with the SEM in order to confirm the accuracy of the positioning of analytical SIMS pits (Figures 4(C,D) and 5(C,D)).

Standards

Due to the scarcity of appropriate reference standards for calibrating the carbon isotopic compositions of chert-permineralized carbonaceous microfossils, this study began with analyses of three new potential standard mounts prepared from carbonaceous chert samples of the ∼3,350 Ma Fig Tree Group collected near Lows Creek in eastern Transvaal, South Africa and housed in the Precambrian Paleobiology Research Group (PPRG) collections at UCLA (Walter et al. 1983). Standards made from the Fig Tree chert include mount PPRG-215-1/2, as well as two others (FTS-1 and FTS-2) from a sample collected approximately 30 km south of Lows Creek on the southeastern side of the Barberton Greenstone Belt (25°55′S, 31°16′E) and provided to K. H. Williford by M. Van Kranendonk. To establish the suitability of new chert-kerogen standards from natural samples, it is desirable for them to contain carbonaceous matter of a known – and ideally homogenous – carbon isotope composition, yield a carbon secondary ion signal intensity within the same dynamic range as that found within fossiliferous cherts, and come from a geologic unit with a well-characterized depositional context and thermal maturity. The newly prepared standards each contain three or four rock chips of organic-rich chert centered within a ∼1' round epoxy mount and polished to a <1-µm finish. Multiple $\delta^{13}C_{org}$ measurements were made on the individual rock chips to determine their isotopic homogeneity and thereby establish their suitability for use as SIMS standards. These 'rock chip measurements' were then compared to preexisting Fig Tree chert standard PPRG-215-2a from the original rock collection (Hayes et al. 1983; House et al. 2000; Walter et al. 1983), previously used in SIMS studies of similarly preserved Precambrian microfossils (e.g. House et al. 2000, 2013; Williford et al. 2013) and having an established $\delta^{13}C_{org}$ value of −31.5‰ (Hayes et al. 1983; House et al. 2000).

Raman spectroscopy

Raman spectroscopy was used to document the kerogenous composition and geochemical maturity of each analyzed microfossil as well as those of the associated particulate detrital kerogen (Figure 2). Raman point spectra and 2-D geochemical maps were acquired and used to characterize the spatial relationships between fossil and associated kerogen and the enclosing microcrystalline quartz chert matrix (Figure 2(B,E)). These Raman data were acquired at the Raman Laboratory of UCLA's Center for the Study of Evolution and the Origin of Life using a T64000 triple-stage confocal laser-Raman system equipped with an argon ion laser having an excitation wavelength of 457.9 nm, a spectral window centered at ∼1700 cm^{-1} and a ∼1 µm spot size. Two-dimensional Raman geochemical maps were acquired across a ∼20 × 20-µm area at 0.5–2.0 µm depth. Spectra here shown (Figure 2(C,F)) are normalized to the intensity of the G-band of kerogen.

Raman geothermometry calculations were performed to provide an estimate of peak metamorphic temperatures. Processed Raman spectra of kerogen were deconvoluted using the method described by Kouketsu et al. (2014) with the software package PeakFit (v.4.12; SeaSolve Software Inc., Massachusetts, U.S.A.) using their 'fitting G' for low-grade carbonaceous matter of the Gaoyuzhuang and Kwagunt Formations, and 'fitting D' and 'fitting B' for the PPRG-215-1 and FTS-1 standards, respectively. From these deconvoluted spectra, approximate peak metamorphic temperatures were calculated using the equation

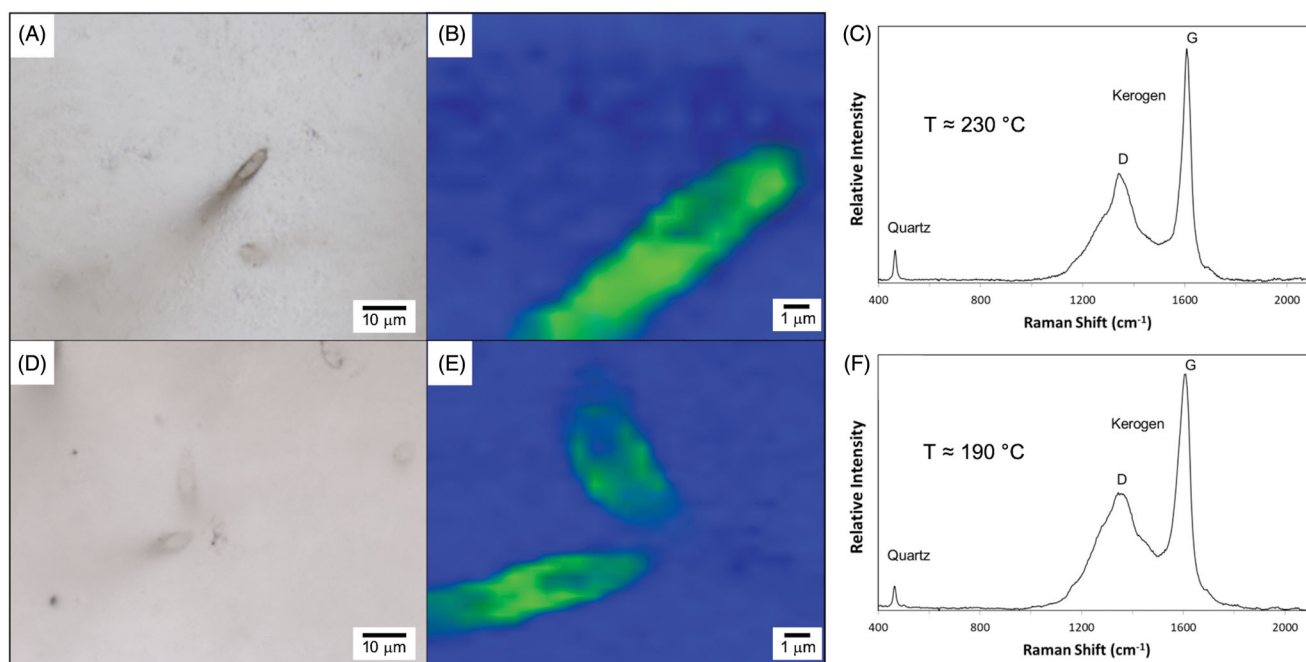$$T(°C) = -2.15(FWHM - D1) + 478$$

(1)

Figure 2. Representative transmitted light photomicrographs (A, D), 2-D Raman images (B, E), and Raman spectra (C, F; normalized to the kerogen G-band) of typical fossil filaments from the Gaoyuzhuang (A, B, C) and Kwagunt (D, E, F) cherts. The 2-D Raman geochemical images (B, E) show the distribution of kerogen comprising the walls of the permineralized fossils (green) relative to the filament-infilling and background quartz matrix (blue). The kerogen Raman spectra (C, F) consist of two bands, the 'disordered' D-band ($\sim$1,350 cm^{-1}) and the 'graphitic' G-band ($\sim$1,600 cm^{-1}), and showing estimated peak metamorphic temperatures; the quartz peak in each spectrum (465 cm^{-1}) is derived from the fossil-encompassing and -infilling chert matrix. Raman images were obtained using a spectral window encompassing the G-band of kerogen, from $\sim$1,575 cm^{-1} to $\sim$1,625 cm^{-1}.

where FWHM-D1 (cm^{-1}) represents the full width at half maximum for the D1 Raman band of carbonaceous matter (i.e. kerogen) centered at 1350 cm^{-1}. This calculation is reliable for temperature measurements in the range of 150–400 °C with an error of ±30 °C (Kouketsu et al. 2014).

Carbon isotope measurements

Bulk carbon isotope analysis

Samples from the Gaoyuzhuang and Kwagunt cherts used in this study had been previously analyzed to determine their 'whole rock' (bulk, 25-g sample) carbon isotope compositions (Strauss et al. 1992b; Strauss and Moore 1992). In the Astrobiogeochemistry Lab at the NASA Jet Propulsion Laboratory (JPL), multiple new δ^{13}C measurements were made of the carbonaceous residues from hydrochloric acid-dissolved rock chips of the Fig Tree chert used to prepare the new reference mounts (FTS-1, FTS-2), the same geologic unit from which the original PPRG-215-1 standard was initially obtained (Hayes et al. 1983; House et al. 2000). Rock chip samples of black chert ($\sim$5 g) were powdered and treated in 6 N HCl for 72 h at 60 °C, with the acid being replaced twice after 24 h. The carbon abundances of the resulting residues were prepared for analysis via combustion and automated, preparative chemistry using a Costech 4010 Elemental Analyzer, and their total organic carbon (TOC) and δ^{13}C$_{org}$ values measured by a coupled Thermo Delta V Plus isotope-ratio mass spectrometer. TOC was calculated by comparing the integrated area under peaks for m/z 44, 45, and 46 ions in the samples with those from multiple

analyses of acetanilide reference material (having a known total carbon abundance) acquired during the same sequence.

SIMS carbon isotope analysis

SIMS carbon isotope measurements were performed during two analytical sessions (5/25/2018 and 1/9–1/14/2019) on the CAMECA IMS-1290 at UCLA using multicollection mode with ^{12}C$_2^-$ detected on a Faraday cup and ^{12}C^{13}C$^-$ detected using an electron multiplier at a mass resolution of $\sim$6,000 that resulted in the separation of molecular hydride interferences. A 20 keV, $\sim$1–2 nA ^{133}Cs$^+$ primary ion beam was focused to a 10 μm spot size; a 5 × 5 μm raster in combination with 100% dynamic transfer was used during the measurements to reduce the down-pit isotope fractionation. Each analysis included 45 s of presputtering and a total counting time of 240 s over 20 measurement cycles. Count rates determined with the electron multiplier were corrected for deadtime (65 ns) and Faraday cup signals were corrected for background levels determined for each analysis by deflecting the secondary ion beam out of the Faraday cup during presputtering.

Multiple measurements of the chert-kerogen standard were used to bracket groups of 15–20 analyzed specimens. The small size of the analyzed fossil filaments (many $\sim$2–4 μm in diameter) compared to the diameter of the analytical spot ($\sim$10 μm) yielded low ion count rates and lower precision compared to larger and/or better exposed fossils and more carbon-rich areas of the chert matrix. Microfossil analyses having low relative count rates (^{12}C$_2^-$$_{rel}$, %) below $\sim$7%, were noted although there was no observed correlation between δ^{13}C$_{org}$ and ^{12}C$_2^-$$_{rel}$ values for accepted

sample analyses, with the exception of some kerogen-poor background measurements (Table S1; Figures S1 and S2, Supplemental Material). Analyses of associated detrital kerogen typically had low relative count rates due to the sparse distribution of particulate organic matter in the analyzed cherts, and thus the $\delta^{13}C_{org}$ values for background kerogen are here included in the data presented despite having relatively low internal precision.

Instrumental bias (α_{SIMS}) was determined by calculating the average 'raw' value ($\delta^{13}C_{raw} = [(^{12}C^{13}C/^{12}C^{12}C)_{measured}/(0.01118 \times 2) - 1] \times 1000$) using the revised $^{13}C/^{12}C$ ratio of 0.01118 for VPDB (Beerling 2001; Chang and Li 1990; Farquhar and Lloyd 1993), for 5 to 8 bracketing analyses of the working standard (PPRG-215-1/2 or FTS-1) compared to its average carbon isotopic ($\delta^{13}C_{bulk}$) value (PPRG-215-1/2 = −31.5‰, Hayes et al. 1983; FTS-1 = −13.5‰, this study), following the method described by Kita et al. (2009) and Williford et al. (2013):

$$\alpha_{SIMS} = (\delta^{13}C_{raw} + 1000)/(\delta^{13}C_{bulk} + 1000).$$

(2)

The α_{SIMS} value thus obtained permits the correction of raw $\delta^{13}C$ values for unknown sample analyses using a second equation (Williford et al. 2013):

$$\delta^{13}C_{VPDB}(sample) = [(1 + \delta^{13}C_{raw}(sample)/1000/\alpha_{SIMS} - 1] \times 1000.$$

(3)

Following the methods established by previous SIMS studies of kerogenous microfossils (e.g. House et al. 2013; Schopf et al. 2018; Williford et al. 2013), external precision (i.e. reproducibility) was calculated as two standard deviations (±2SD) of the $\delta^{13}C_{raw}$ values obtained for the bracketing measurements of the standard. Internal precision was calculated as two standard errors (±2SE) of $\delta^{13}C_{raw}$ values measured over 20 individual cycles for each SIMS analysis, results largely influenced by the heterogeneity in abundance of organic carbon at depth within the target area affecting counting statistics.

Results

Over the course of the two SIMS analytical sessions, a total of 307 analyses were made including 241 measurements of the chert-kerogen reference standards and 66 measurements of target-sample microfossils and associated particulate kerogen. In general, the standards exhibited greater secondary ion intensities ($>1.5 \times 10^6$ cps, counts per second for $^{12}C^{12}C^-$) and more isotopic homogeneity (± ∼1.5–3.5‰; 2SD) than the samples. The large number of measurements performed in this study enabled detailed evaluation of the newly prepared reference standards for their suitability as chert-kerogen standards in SIMS $\delta^{13}C_{org}$ analyses, and for comparison of the variation among carbon isotope signatures preserved in carbonaceous microfossils chert-

permineralized in two temporally and spatially disparate Proterozoic marine ecosystems. Raman spectra of quartz and kerogen in the samples and standards demonstrate the similarities in their geochemical composition. The FTS-1 mount was used as the primary working standard during SIMS sample analyses, and the instrumental mass fractionation (IMF, ‰) for this standard averaged −15.2‰ during the first session ($n = 18$) and −14.3‰ for the second session ($n = 81$). The IMF determined for the other chert-kerogen standards measured during the second session are within ∼2‰ of the average value for FTS-1. These data indicate that any matrix effects arising from chemical and/or mineralogical differences between the samples and standards during SIMS analysis are minimal. Raman geothermometry calculations for kerogen show a large difference in estimated peak metamorphic temperatures between the samples and the standards, and between the two isotopically distinct standards. Kerogen in the Gaoyuzhuang Formation cherts has an approximate peak temperature of ∼230 ± 30 °C, and the Kwagunt Formation samples have a similar estimated value of ∼190 ± 30 °C. Peak temperatures for the standards are estimated to be much higher, with the PPRG-215 sample producing an average of ∼375 ± 30 °C, and the FTS-1 sample reaching temperatures greater than 400 °C (Table S2; Figure S3, Supplemental Material).

Chert-kerogen standards

The original Fig Tree chert standard (PPRG-215-2a) and the newly prepared mount from the same rock (PPRG-215-1/2) analyzed in this study ($n = 114$) had consistent $^{12}C^{13}C/^{12}C^{12}C$ ratios (±1.5–3.5‰; 2SD) and an experimental bias (i.e. instrumental mass fractionation) of roughly −14 to −16‰ with an average $^{12}C_2^-$ count rate of 1.8×10^6 cps. The two additional newly prepared Fig Tree chert standards (FTS-1, FTS-2; $n = 127$) are isotopically distinct from the PPRG-215 standards (PPRG-215-2a, PPRG-215-1/2), offset by ∼18‰, a difference consistent with $\delta^{13}C_{org}$ data obtained from bulk measurements of the FTS standards which yielded an average of −13.52‰ ± 0.03 ($n = 4$). SIMS analyses of the FTS standards yielded similarly consistent $\delta^{13}C$ values (±1.4–2.3‰; 2SD) with an experimental bias ranging from ∼14–16‰ and an average $^{12}C_2^-$ count rate of 2.3×10^6 cps. External precision (2SD) averaged ∼2.7‰ and ∼2.0‰ for all accepted analyses of the PPRG-215 and FTS mounts, respectively, and external precision for bracketing measurements ranged from ∼1.1‰ to ∼1.5‰ with minimal instrument drift and consistent α_{SIMS} values ranging from ∼0.984–0.986 (Table S1, Supplemental Material). Average internal precision (2SE) was ∼1.3‰ for the PPRG standards and ∼1.2‰ for the FTS standards. To avoid overestimation of errors and better reflect variations in isotopic compositions and $^{12}C_2^-$ count rates within one spot, total uncertainty (i.e. final error) is expressed as the square root of the sum of the squares for the standard error of the mean for the bracketing measurements and the internal precision of each sample analysis (Table S1, Supplemental Material). SIMS measurements having $^{12}C_2^-$ count rates below
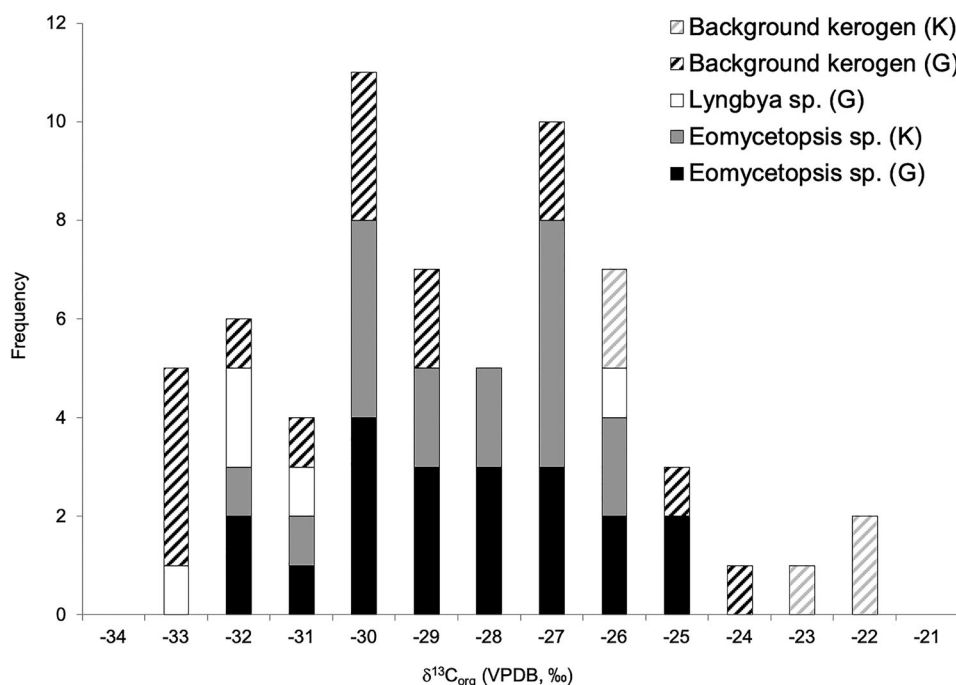
Figure 3. Histogram of SIMS carbon isotope data for samples from the Gaoyuzhuang (G) and Kwagunt (K) Formations, with $\delta^{13}C_{org}$ values placed into 1‰ bins. Solid bars (black, gray, white) represent microfossil analyses, and dashed bars (black, gray) show distribution of SIMS data for associated background kerogen.

2.0×10^5 cps were discarded from the data, with the exception of background particulate kerogen analyses of the samples. As shown in Table S2 (Supplemental Material), the new bulk measurements showed that the total organic carbon (TOC) values for the FTS samples were consistently $\sim$0.45 mg/g, compared to $\sim$1.40 mg/g from previous measurements of the whole-rock PPRG-215 samples (Hayes et al. 1983).

Microfossil samples

The $\delta^{13}C_{org}$ values of the SIMS target samples, fossils and associated background kerogen, ranged from -33.8‰ to -22.4‰, with an average count rate of 8.5×10^5 (cps) (Figure 3; Table S1, Supplemental Material). Gaoyuzhuang microfossils ($n = 34$; Figure 4) had an average $\delta^{13}C_{org}$ of -29.4 ± 2.5‰, the associated particulate kerogen measuring on average -30.3 ± 2.9‰ ($n = 15$). Values for 2–4 μm-wide Gaoyuzhuang *Eomycetopsis* fossils averaged -28.9 ± 2.2‰ whereas the broader, 30–40 μm-diameter *Lyngbya*-like tubules from the unit had an average $\delta^{13}C_{org}$ value of -31.2 ± 2.9‰ ($n = 5$). Average internal precision (2SE) for all measurements of the Gaoyuzhuang samples was $\sim$1.9‰, and the average $^{12}C_2^-$ count rate was $\sim$7.5 $\times 10^5$ cps. *Eomycetopsis* microfossils from the Kwagunt Formation ($n = 17$; Figure 5) yielded an average $\delta^{13}C_{org}$ of -29.0 ± 1.8‰, and the average for background kerogen was -24.3 ± 1.9‰ ($n = 5$); however, the background measurements yielded notably low count rates ($^{12}C_2^-{}_{rel}$ below 7%). Average internal precision for all measurements of the Kwagunt samples was 2.1‰, and the average $^{12}C_2^-$ count rate was $\sim$1.0 $\times 10^6$ cps.

Discussion

Filamentous microfossils permineralized in carbonaceous cherts of the $\sim$1,560 Ma Gaoyuzhuang Formation of northern China and $\sim$850 Ma Kwagunt Formation of Arizona, U.S.A. share very similar morphological and preservational characteristics despite being widely separated in both space and time, the comparability of their microbial components attributable to the extremely slow evolution of Precambrian cyanobacteria. Although previous paleobiological studies and bulk carbon isotope analyses of organic matter from these deposits firmly implicated the photoautotrophic composition of the two communities, it has been only recently that the combination of morphological, geochemical, and isotopic analyses of individual microfossils has been available to validate these interpretations. Using optical microscopy, Raman spectroscopy, and SIMS to analyze, respectively, the morphological, geochemical, and isotopic composition of the fossils, the data here presented substantiate their earlier proposed taxonomic assignments and provide new means to interpret their metabolic characteristics.

Chert-kerogen standards

Despite having been collected from the same geological unit, rock chip measurements of two of the newly prepared Fig Tree chert-kerogen reference standards for SIMS carbon isotope studies (FTS-1, FTS-2) differ significantly from those of the originally used PPRG-215 sample (PPRG-215-2a) and the second mount prepared from the same collection (PPRG-215-1/2). Whereas the two PPRG samples yielded bulk $\delta^{13}C_{org}$ values of approximately -31.5‰, the new FTS standards – collected at a more metamorphosed locality than that originally sampled – were relatively enriched in
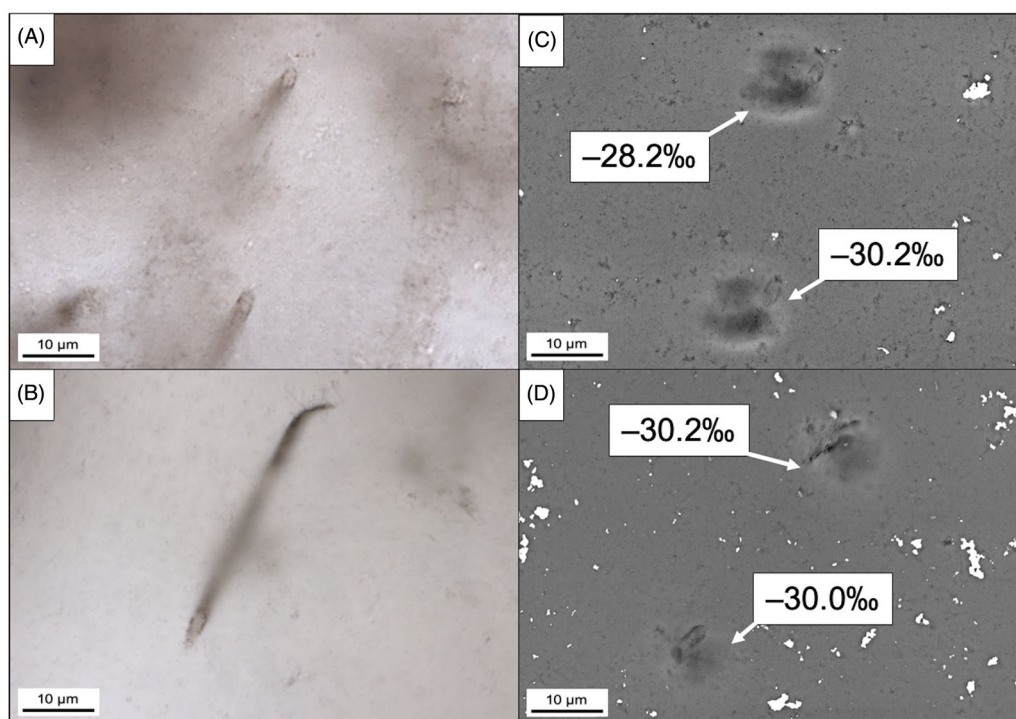
Figure 4. Transmitted light (left) and backscattered electron (right) images of representative *Eomycetopsis* specimens from the Gaoyuzhuang chert analyzed with SIMS at the thin section surface showing the $\delta^{13}C_{org}$ values (‰) measured in the ~10 μm-diameter analytical pits.
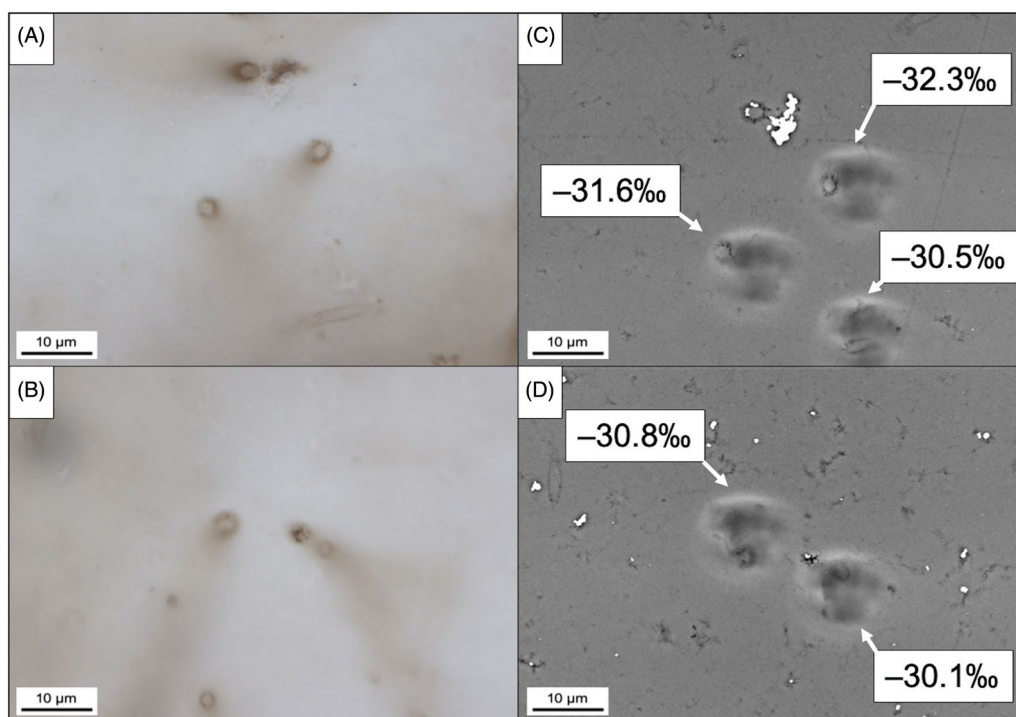

Figure 5. Transmitted light (left) and backscattered electron (right) images of representative *Eomycetopsis* specimens from the Kwagunt chert analyzed with SIMS at the thin section surface showing the $\delta^{13}C_{org}$ values (‰) measured in the ~10 μm-diameter analytical pits.

^{13}C by ~18‰, having an average value of −13.5‰. Raman spectroscopy analyses of the kerogen in the two sets of standards similarly showed a difference in the geochemical maturity of their kerogenous components consistent with their geologic settings, those in the FTS samples being appreciably more heated and geochemically altered (Figure S3, Supplemental Material). These results are supported by

previously reported Raman data from thermally altered kerogens within the variably metamorphosed Barberton Greenstone Belt (Tice et al. 2004).

It should be noted, however, that despite the marked differences between the two sets of standards, in SIMS analyses of Precambrian microfossils the use of two isotopically (and geothermally) distinct standards is potentially valuable, the

combination of the differing data sets providing two-point calibration, a technique that has been suggested to improve the reliability of stable isotope measurements and their subsequent interpretation (Jardine and Cunjak 2005). As this investigation represents the first SIMS study of microfossils to employ two suitable carbonaceous chert standards of differing isotopic compositions, a simple calibration using all of the accepted standard analyses from the second SIMS session ($n = 218$) was applied to the raw $\delta^{13}C$ values measured for unknown samples during that session ($\delta^{13}C_{VPDB}$(calibrated) $= 0.9561 \times \delta^{13}C_{raw} + 13.069$). This calculation yields comparable $\delta^{13}C_{org}$ values within $\sim$1–2‰ to those calculated from equation 3 described above, and a similar internal precision of $\sim$2.3‰ (2SE; standard error of the regression).

SIMS carbon isotope analyses

The $\delta^{13}C_{org}$ values of *Eomycetopsis* sp. specimens from the Gaoyuzhuang (average $= -28.9‰$) and Kwagunt cherts (average $= -29.0‰$) are indistinguishable despite their notable separation in space and time, a similarity consistent with the marked comparability of their filamentous morphologies, shallow-marine depositional settings, and with the known evolutionary history of oscillatoriacean cyanobacteria. The $\delta^{13}C_{org}$ values of the Gaoyuzhuang *Lyngbya*-like sheaths ($-31.2‰$) are also within the range of the smaller *Eomycetopsis* filaments in both units, albeit some 2‰ lower on average, with the measured values and calculated fractionations of all specimens falling within the range determined for modern microbial phototrophs (e.g. Orphan and House 2009; Schidlowski 2001; Zerkle et al. 2005) as well as within the ranges reported for other SIMS-analyzed Precambrian cyanobacterial fossils, including spheroidal and ellipsoidal microfossils from the Gaoyuzhuang Formation (Peng et al. 2016). Such carbon isotope fractionations are consistent with autotrophic carbon fixation through the Calvin cycle using RuBisCO (cf., House et al. 2000). Many earlier SIMS studies appropriately stressed the importance of interpreting stable carbon isotope values (and fractionations) from Precambrian fossils and host rocks in their proper geological, paleobiological, and preservational context. These factors, which largely control the final isotopic composition of fossil kerogens, are discussed below.

Carbon isotopes of Proterozoic microfossils

The $\delta^{13}C_{org}$ composition of Precambrian sedimentary kerogen is primarily determined by the biosynthetic processes involved in its formation; however, modern microorganisms kinetically fractionate carbon isotopes to differing extents depending on the type of metabolism (e.g. Hayes 2001; Schidlowski 2001; Zerkle et al. 2005). Given this, the sedimentary $\delta^{13}C_{org}$ record has been used to infer ancient carbon fixation pathways and explore the biogeochemical carbon cycle of the early Earth (Des Marais 1997; Hayes et al. 1999; Schidlowski 2001), including physiological interpretations of silicified Precambrian microfossils (e.g. House et

al. 2000, 2013; Peng et al. 2016; Williford et al. 2013) similar to those investigated here.

In addition to metabolism, the $\delta^{13}C_{org}$ value of modern microorganisms and preserved microfossils is affected by the isotopic composition of their inorganic carbon source (e.g. $CO_{2(aq)}$ or HCO_3^-), including deposits within the relatively inconstant shallow-marine photic zone such as those here studied. It has also been shown that extant cyanobacteria are capable of using either dissolved CO_2 or HCO_3^- (Badger and Price 2003), processes that would presumably result in differing isotopic compositions for biomass. Although it is generally assumed that the ocean–atmosphere and inorganic pools of CO_2 and HCO_3^- were in thermodynamic equilibrium (with equilibrium isotopic fractionation) throughout the Proterozoic (e.g. Kaufman and Xiao 2003; Schidlowski 2001), the concentration of CO_2 has been highlighted for its simplicity in interpreting isotopic fractionations (e.g. House et al. 2000; Williford et al. 2013) and the capability of cyanobacteria to use HCO_3^- is thought to be a more recent development and/or rare occurrence – perhaps evolved as a response to lower atmospheric CO_2 concentrations (Badger and Price 2003; Nisbet et al. 2007). The $\delta^{13}C_{carb}$ composition of most sedimentary carbonates therefore likely records the $\delta^{13}C$ of dissolved inorganic carbon (DIC) available to ancient microorganisms and thus the difference between $\delta^{13}C_{carb}$ and $\delta^{13}C_{org}$ values can be used to estimate total metabolic fractionations ($\Delta^{13}C = \delta^{13}C_{DIC} - \delta^{13}C_{org}$) (Williford et al. 2013). This relationship is further expanded using the following equation (Hayes et al. 1999):

$$\Delta^{13}C_{carb-org} = \Delta_{carb} + \varepsilon_p - \Delta_2 \qquad (4)$$

in which Δ_{carb} represents the equilibrium isotope fractionation between sedimentary carbonate and dissolved $CO_{2(aq)}$, which is temperature-dependent and ranges from $\sim$7‰ at 30 °C to 10.4‰ at 0 °C, assuming an isotopic composition of calcium carbonate minerals (e.g. calcite, $CaCO_3$) relative to DIC (e.g. bicarbonate, HCO_3^-) that is lower by $\sim$1.2‰ (Hayes et al. 1999). The value for kinetic isotope fractionation associated with autotrophic biosynthesis (ε_p) is the greatest contributing factor affecting the primary $\delta^{13}C_{org}$ composition of recently deposited organic matter and the later formation of fossil kerogen. Secondary alteration (Δ_2) represents the isotope effect(s) due to post-depositional processes that alter the initial carbon isotope signature, including decomposition, heterotrophic degradation and thermal alteration due to burial and metamorphism.

For extant photoautotrophic microbes, isotope fractionation due to carbon fixation ($\varepsilon_p = \delta^{13}C_{substrate} - \delta^{13}C_{fixed\ carbon}$) is dependent on environmental and physiological factors not only including dissolved CO_2 concentrations but also nutrient availability, cell geometry and growth rate (e.g. Cassar et al. 2006; Guy et al. 1993; Laws et al. 1995, 1997; Popp et al. 1998). Laboratory studies show that ε_p for the carboxylation of RuBisCO by cyanobacteria has a typical range of $\sim$16–22‰ (e.g. Guy et al. 1993; Popp et al. 1998) and a potential maximum fractionation of $\sim$25‰ (e.g. Kaufman and Xiao 2003), compared to phototrophic eukaryotes which have ε_p values up to 32‰ (Roeske and O'Leary 1985; Hayes et al. 1999). Given

these considerations, the $\delta^{13}C_{org}$ values measured for the *Eomycetopsis* specimens of the Gaoyuzhuang and Kwagunt cherts approach the maximum estimated ε_p for cyanobacteria, considering most of the $\delta^{13}C_{carb}$ values for these units are between $-1‰$ and $+1‰$ and assuming the surface ocean temperatures were 15–30 °C (e.g. Garcia et al. 2017; Knauth 2005). This suggests the shallow-marine *Eomycetopsis* populations were not limited by low $CO_{2(aq)}$ concentrations or high growth rates, conditions which tend to lower ε_p values in laboratory studies (e.g. Laws et al. 1995, 1997).

In the two deposits studied here, a significant role of secondary alteration affecting preserved isotopic ratios is ruled out by the Raman spectra obtained both for the microfossil-comprising kerogen and the kerogen of the associated background organic matter. Comparing the Raman spectra of the Gaoyuzhuang and Kwagunt microfossils (Figure 2) with previously reported data (e.g. Kouketsu et al. 2014; Schopf et al. 2005), it is apparent that the microfossils are composed of thermally immature kerogen – below greenschist facies – and that geochemical thermal alteration can be essentially excluded for the specimens studied here (Schidlowski 2001; Schiffbauer et al. 2012).

The role of heterotrophic recycling by post-depositional biodegradation might also be considered as a possible factor affecting the isotopic composition of fossil kerogen. Measurements of background associated detrital kerogen in the Gaoyuzhuang samples, yielding $\delta^{13}C_{org}$ values $(-30.3 \pm 2.9‰)$ similar to previous bulk measurements (ca. -28 to $-31‰$) for this unit, are well within the range of values for the microfossils $(-29.4 \pm 2.5‰)$, suggesting that the fossils and associated organic matter probably share a common biosynthetic origin. In contrast, although the Kwagunt $\delta^{13}C_{org}$ analyses for such subsidiary kerogen $(-24.3 \pm 1.9‰)$ suffer from relatively low count rates, they are more similar to bulk measurements of whole-rock specimens (ca. -24 to $-26‰$), which are ~3–$5‰$ higher than the values measured for the *Eomycetopsis* fossils $(-29.0 \pm 1.8‰)$. This difference, though relatively small, could represent deposition of recycled exogenous organic matter (Johnston et al. 2012) or it may reflect the occurrence of degradation by co-existing heterotrophs, perhaps marine protozoans or early-evolved soft-bodied metazoans (the Kwagunt dating from ~850 Ma) as the cyanobacterial sheaths were selectively preserved (Bartley 1996). DeNiro and Epstein (1978) classically stated, 'You are what you eat (plus a few ‰),' describing the isotopic effects of heterotrophic alteration on the primary biomass or food source. Whereas thermal alteration can potentially increase $\delta^{13}C_{org}$ values $>10‰$ in highly metamorphosed rocks (Schidlowski 2001) – as shown here by the 18‰ offset between the two sets of SIMS standards – the effects of heterotrophic recycling are unlikely to exceed $\sim5‰$ in marine settings (Hayes 1993) and would require a much larger sample size to properly establish in the Proterozoic rock record.

Biological affinities of microfossils

Analyses of ^{13}C-depleted carbon in kerogenous organic matter, even for specific microfossils, may not be directly indicative of biological affinities. Like carbon fixation within the Calvin cycle, other cellular metabolisms, such as the acetyl-CoA pathway (Fuchs et al. 1979; Preuβ et al. 1989; Schidlowski et al. 1983) have been shown to kinetically fractionate carbon isotopes to comparable magnitudes. Nevertheless, the combination of shared morphological features and similar $\delta^{13}C_{org}$ values among the filamentous microfossils studied here, and their notable similarity to extant and other fossil microbial phototrophs, as well as their demonstrable occurrence in the photic zone of shallow-marine environments, all firmly support their classification as oxygen-producing cyanobacteria, photoautotrophs utilizing the Calvin cycle responsible for their characteristic $\delta^{13}C_{org}$ values. The available data thus support and corroborate the previous taxonomic oscillatoriacean cyanobacterial assignment of the *Eomycetopsis* and *Lyngbya*-like microfossils of the Gaoyuzhuang and Kwagunt Formations (e.g. Schopf et al. 1973, 1984).

An alternative explanation for the similar $\delta^{13}C_{org}$ values – and interpretation of the microfossil physiologies – is that they may represent facultative oxygenic–anoxygenic cyanobacteria (e.g. Cohen et al. 1975, 1986). Among extant oscillatoriaceans this is a relatively widespread capability (e.g. Padan 1979) that reflects the derivation of the cyanobacterial lineage from anoxygenic photosynthetic bacteria, which should have remained prevalent in the Proterozoic oceans (Johnston et al. 2009). Affinities with other early-evolved lineages, particularly methanogens, methanotrophs, and sulfur- or sulfate-reducing microbes can be effectively ruled out due to a combination of differences in morphology, metabolisms, isotopic signatures and/or depositional setting.

The findings of this study contribute to the increase in data obtained for SIMS $\delta^{13}C_{org}$ analyses of carbonaceous Precambrian microfossils and illustrates the potential for indistinguishable carbon isotope values to be preserved within samples sharing distinct morphological and depositional similarities, despite being widely separated in both space and time. Using additional data from carbon isotope measurements of inorganic carbon ($\delta^{13}C_{carb}$) and Raman spectroscopy, the possibility of reconstructing ancient carbon fixation pathways for these filamentous microfossils has become further constrained by in situ SIMS analyses, and in conclusion documents the ubiquity, persistence, and extremely slow evolution of oxygen-producing oscillatoriacean cyanobacteria, dominant components of shallow water photic zone environments throughout much of Earth's Precambrian history.

Acknowledgements

Disclosure statement

Funding

ORCID

Jeffrey T. Osterhout 🔾 http://orcid.org/0000-0001-8523-0072

References

Anbar AD, Duan Y, Lyons TW, Arnold GL, Kendall B, Creaser RA, Kaufman AJ, Gordon GW, Scott C, Garvin J, et al. 2007. A whiff of oxygen before the Great Oxidation Event? Science. 317(5846): 1903–1906.

Awramik SM. 1992. The oldest records of photosynthesis. Photosynth Res. 33(2):75–89.

Awramik SM, Schopf JW, Walter MR. 1983. Filamentous fossil bacteria from the Archean of Western Australia. In: Nagy B, Weber R, Guerrero JC, Schidlowski M, editors. Developments in Precambrian Geology. Amsterdam: Elsevier, p249–266.

Badger MR, Price GD. 2003. CO_2 concentrating mechanisms in cyano-bacteria: molecular components, their diversity and evolution. J Exp Bot. 54(383):609–622.

Bartley JK. 1996. Actualistic taphonomy of cyanobacteria: implications for the Precambrian fossil record. Palaios. 11(6):571–586.

Beerling DJ. 2001. Carbon isotopes in plants. In: Briggs DE, Crowther PR, editors. Palaeobiology II. Oxford: Blackwell Publishing Ltd, p473–475.

Bloeser B. 1985. Melanocyrillium, a new genus of structurally complex late Proterozoic microfossils from the Kwagunt Formation (Chuar Group), Grand Canyon, Arizona. J Paleontol. 59:741–765.

Bosak T, Liang B, Sim MS, Petroff AP. 2009. Morphological record of oxygenic photosynthesis in conical stromatolites. PNAS. 106(27): 10939–10943.

Buick R. 1992. The antiquity of oxygenic photosynthesis: evidence from stromatolites in sulphate-deficient Archaean lakes. Science. 255(5040):74–77.

Buick R. 2008. When did oxygenic photosynthesis evolve? Phil Trans R Soc B. 363(1504):2731–2743.

Burns BP, Goh F, Allen M, Neilan BA. 2004. Microbial diversity of extant stromatolites in the hypersaline marine environment of Shark Bay, Australia. Appl Environ Microbiol. 6:1096–1101.

Butterfield NJ. 2015. Proterozoic photosynthesis–a critical review. Palaeontol. 58(6):953–972.

Cassar N, Laws EA, Popp BN. 2006. Carbon isotopic fractionation by the marine diatom Phaeodactylum tricornutum under nutrient- and light-limited growth conditions. Geochim Cosmochim Acta. 70(21): 5323–5335.

Chang T, Li W. 1990. A calibrated measurement of the atomic weight of carbon. Chinese Sci Bull. 35:290–296.

Chu X, Zhang T, Zhang Q, Feng L, Zhang F. 2004. Carbon isotopic variations of Proterozoic carbonates in Jixian. Sci China Ser D-Earth Sci. 47(2):160–170.

Chu X, Zhang T, Zhang Q, Lyons TW. 2007. Sulfur and carbon isotope records from 1700 to 800 Ma carbonates of the Jixian section, northern China: implications for secular isotope variations in Proterozoic seawater and relationships to global supercontinental events. Geochim Cosmochim Acta. 71(19):4668–4692.

Cohen Y, Jorgensen BB, Revsbech NP, Poplawski R. 1986. Adaptation to hydrogen sulfide of oxygenic and anoxygenic photosynthesis among cyanobacteria. Appl Environ Microbiol. 51(2):398–407.

Cohen Y, Jørgensen BB, Padan E, Shilo M. 1975. Sulfide-dependent anoxygenic photosynthesis in the cyanbacterium Oscillatoria limne-tica. Nature. 257(5526):489–492.

DeNiro MJ, Epstein S. 1978. Influence of diet on the distribution of carbon isotopes in animals. Geochim Cosmochim Acta. 42(5): 495–506.

Des Marais DJ. 1997. Isotopic evolution of the biogeochemical carbon cycle during the Proterozoic Eon. Org Geochem. 27(5–6):185–193.

Des Marais DJ. 2001. Isotopic evolution of the biogeochemical carbon cycle during the Precambrian. Rev Mineral Geochem. 43(1): 555–578.

Farquhar GD, Ehleringer JR, Hubick KT. 1989. Carbon isotope dis-crimination and photosynthesis. Annu Rev Plant Physiol Plant Mol Biol. 40(1):503–537.

Farquhar GD, Lloyd J. 1993. Carbon and oxygen isotope effects in the exchange of carbon dioxide between terrestrial plants and the atmosphere. In: Ehleringer JR, Hall AE, Farquhar GD, editors. Stable Isotopes and Plant Carbon-Water Relations. Cambridge (MA): Academic Press, p47–70.

Ford TD, Breed WJ. 1973. Late Precambrian Chuar Group, Grand Canyon, Arizona. Geol Soc America Bull. 84(4):1243–1260.

Fuchs G, Thauer R, Ziegler H, Stichler W. 1979. Carbon isotope frac-tionation by Methanobacterium thermoautotrophicum. Arch Microbiol. 120(2):135–139.

Garcia AK, Schopf JW, Yokobori SI, Akanuma S, Yamagishi A. 2017. Reconstructed ancestral enzymes suggest long-term cooling of Earth's photic zone since the Archean. Proc Natl Acad Sci U S A. 114(18):4619–4624.

Golubic S, Seong-Joo L. 1999. Early cyanobacterial fossil record: preser-vation, palaeoenvironments and identification. Eur J Phycol. 34(4): 339–348.

Grotzinger JP, Knoll AH. 1999. Stromatolites in Precambrian carbo-nates: evolutionary mileposts or environmental dipsticks? Annu Rev Earth Planet Sci. 27:313–358.

Guo H, Du Y, Kah LC, Huang J, Hu C, Huang H, Yu W. 2013. Isotopic composition of organic and inorganic carbon from the Mesoproterozoic Jixian Group, North China: implications for bio-logical and oceanic evolution. Precambrian Res. 224:169–183.

Guy RD, Fogel ML, Berry JA. 1993. Photosynthetic fractionation of the stable isotopes of oxygen and carbon. Plant Physiol. 101(1):37–47.

Hayes JM. Kaplan IR, Wedeking KW 1983. Precambrian organic geo-chemistry, preservation of the record. In: Schopf JW, editor. The Earth's Earliest Biosphere: Its Origin and Evolution. Princeton (NJ): Princeton University Press, p93–134.

Hayes JM, Strauss H, Kaufman AJ. 1999. The abundance of ^{13}C in marine organic matter and isotopic fractionation in the global bio-geochemical cycle of carbon during the past 800 Ma. Chem Geol. 161(1–3):103–125.

Hayes JM. 1993. Factors controlling ^{13}C contents of sedimentary organic compounds: principles and evidence. Mar Geol. 113(1–2): 111–125.

Hayes JM. 2001. Fractionation of carbon and hydrogen isotopes in bio-synthetic processes. Rev Mineral Geochem. 43(1):225–277.

Hofmann HJ. 1976. Precambrian microflora, Belcher Islands, Canada: significance and systematics. J Paleontol. 50:1040–1073.

Hongwei K, Yongqing L, Jiahua L, Nan P, Shunshe L, Chao C. 2011. Carbon and oxygen isotopic stratigraphy of Mesoproterozoic car-bonate sequences (1.6–1.4 Ga) from Yanshan in North China. Int J Oceanogr. 2011:1–11.

House CH, Oehler DZ, Sugitani K, Mimura K. 2013. Carbon isotopic analyses of ca. 3.0 Ga microstructures imply planktonic autotrophs inhabited Earth's early oceans. Geology. 41(6):651–654.

House CH, Schopf JW, McKeegan KD, Coath CD, Harrison TM, Stetter KO. 2000. Carbon isotopic composition of individual Precambrian microfossils. Geology. 8:707–710.

Jardine TD, Cunjak RA. 2005. Analytical error in stable isotope ecology. Oecologia. 144(4):528–533.

Javaux EJ, Lepot K. 2018. The Paleoproterozoic fossil record: implications for the evolution of the biosphere during Earth's middle-age. Earth Sci Rev. 176:68–86.

Johnston DT, Macdonald FA, Gill BC, Hoffman PF, Schrag DP. 2012. Uncovering the Neoproterozoic carbon cycle. Nature. 483(7389): 320–323.

Johnston DT, Wolfe-Simon F, Pearson A, Knoll AH. 2009. Anoxygenic photosynthesis modulated Proterozoic oxygen and sustained Earth's middle age. PNAS. 106(40):16925–16929.

Karlstrom KE, Bowring SA, Dehler CM, Knoll AH, Porter SMD, Marais DJ, Weil AB, Sharp ZD, Geissman JW, Elrick MB, Timmons JM, et al. 2000. Chuar Group of the Grand Canyon: record of breakup of Rodinia, associated change in the global carbon cycle, and ecosystem expansion by 740 Ma. Geol. 28(7):619–622.

Kaufman AJ, Johnston DT, Farquhar J, Masterson AL, Lyons TW, Bates S, Anbar AD, Arnold GL, Garvin J, Buick R. 2007. Late Archean biospheric oxygenation and atmospheric evolution. Science. 317(5846):1900–1903.

Kaufman AJ, Xiao S. 2003. High CO$_2$ levels in the Proterozoic atmosphere estimated from analyses of individual microfossils. Nature. 425(6955):279–282.

Kita NT, Ushikubo T, Fu B, Valley JW. 2009. High precision SIMS oxygen isotope analysis and the effect of sample topography. Chem Geol. 264(1–4):43–57.

Klein C, Beukes NJ, Schopf JW. 1987. Filamentous microfossils in the early Proterozoic Transvaal Supergroup: their morphology, significance, and paleoenvironmental setting. Precambrian Res. 36(1): 81–94.

Knauth LP. 2005. Temperature and salinity history of the Precambrian ocean: implications for the course of microbial evolution. Palaeogeogr Palaeoclimatol Palaeoecol. 219(1–2):53–69.

Knoll AH, Swett K, Burkhardt E. 1989. Paleoenvironmental distribution of microfossils and stromatolites in the Upper Proterozoic Backlundtoppen Formation. J Paleontol. 63(2):129–145.

Knoll AH. 1985a. Patterns of evolution in the Archean and Proterozoic eons. Paleobiology. 11(1):53–64.

Knoll AH. 1985b. The distribution and evolution of microbial life in the Late Proterozoic era. Annu Rev Microbiol. 39:391–417.

Knoll AH. 2012. The fossil record of microbial life. In: Knoll AH, Canfield DE, Konhauser KO, editors. Fundamentals of Geobiology. Hoboken (NJ): Wiley, p297–314.

Kouketsu Y, Mizukami T, Mori H, Endo S, Aoya M, Hara H, Nakamura D, Wallis S. 2014. A new approach to develop the Raman carbonaceous material geothermometer for low-grade metamorphism using peak width. Isl Arc. 23(1):33–50.

Kremer B, Kazmierczak J, Lukomska-Kowalczyk M, Kempe S. 2012. Calcification and silicification: fossilization potential of cyanobacteria from stromatolites of Niuafo'ou's Caldera Lakes (Tonga) and implications for the early fossil record. Astrobiology. 12(6):535–548.

Laws EA, Bidigare RR, Popp BN. 1997. Effect of growth rate and CO$_2$ concentration on carbon isotopic fractionation by the marine diatom Phaeodactylum tricornutum. Limnol Oceanogr. 42(7):1552–1560.

Laws EA, Popp BN, Bidigare RR, Kennicutt MC, Macko SA. 1995. Dependence of phytoplankton carbon isotopic composition on growth rate and $[CO_2]_{aq}$: theoretical considerations and experimental results. Geochim Cosmochim Acta. 59(6):1131–1138.

Li HK, Zhu SX, Xiang ZQ, Su WB, Lu SN, Zhou HY, Geng JZ, Li S, Yang FJ. 2010. [Zircon U–Pb dating on tuff bed from Gaoyuzhuang Formation in Yanqing, Beijing: further constraints on the new subdivision of the Mesoproterozoic stratigraphy in the northern North China Craton]. Acta Petrol Sin. 26:2131–2140. [Chinese]

Lu SN, Li HM. 1991. A precise U-Pb single zircon age determination for the volcanics of Dahongyu Formation, Changcheng System in Jixian. Bull Chinese Acad Geol Sci. 22:137–145. [Chinese]

Meng QR, Wei HH, Qi YQ, Ma SX. 2011. Stratigraphic and sedimentary records of the rift to drift evolution of the northern North China craton at the Paleo- to Mesoproterozoic transition. Gondwana Res. 20(1):205–218.

Moore TB, Schopf JW. 1992. Geographic and geologic data for PPRG rock samples. In: Schopf JW, Klein C, editors. The Proterozoic Biosphere, a Multidisciplinary Study. Cambridge (UK): Cambridge University Press, p603–693.

Nisbet EG, Grassineau NV, Howe CJ, Abell PI, Regelous M, Nisbet RER. 2007. The age of Rubisco: the evolution of oxygenic photosynthesis. Geobiology. 5(4):311–335.

Oehler DZ, Walsh MM, Sugitani K, Liu M-C, House CH. 2017. Large and robust lenticular microorganisms on the young Earth. Precambrian Res. 296:112–119. doi:10.1016/j.precamres.2017.04.031.

Orphan VJ, House CH. 2009. Geobiological investigations using secondary ion mass spectrometry: microanalysis of extant and paleomicrobial processes. Geobiology. 7(3):360–372.

Padan E. 1979. Facultative anoxygenic photosynthesis in cyanobacteria. Annu Rev Plant Physiol. 30(1):27–40.

Peng X, Guo Z, House CH, Chen S, Ta K. 2016. SIMS and NanoSIMS analyses of well-preserved microfossils imply oxygen-producing photosynthesis in the Mesoproterozoic anoxic ocean. Chem Geol. 441:24–34.

Popp BN, Laws EA, Bidigare RR, Dore JE, Hanson KL, Wakeham SG. 1998. Effect of phytoplankton cell geometry on carbon isotopic fractionation. Geochim Cosmochim Acta. 62(1):69–77.

Preuβ A, Schauder R, Fuchs G, Stichler W. 1989. Carbon isotope fractionation by autotrophic bacteria with 3 different CO$_2$ fixation pathways. Z Naturforsch C J Biosci. 44:397–402.

Reid RP, Visscher PT, Decho AW, Stolz JF, Bebout BM, Dupraz C, Macintyre IG, Paerl HW, Pinckney JL, Prufert-Bebout L, et al. 2000. The role of microbes in accretion, lamination and early lithification of modern marine stromatolites. Nature. 406(6799):989–992.

Roeske CA, O'Leary MH. 1985. Carbon isotope effect on carboxylation of ribulose bisphosphate catalyzed by ribulose bisphosphate carboxylase from Rhodospirillum rubrum. Biochemistry. 24(7): 1603–1607.

Schidlowski M, Hayes J, Kaplan I. 1983. Isotopic inferences of ancient biochemistries: carbon, sulfur, hydrogen, and nitrogen. In: Schopf JW, editor. Earth's Earliest Biosphere, its Origin and Evolution. Hoboken (NJ): Princeton University Press, p149–185.

Schidlowski M. 2001. Carbon isotopes as biogeochemical recorders of life over 3.8 Ga of Earth history: evolution of a concept. Precambrian Res. 106(1–2):117–134.

Schiffbauer JD, Wallace AF, Hunter JL, Jr, Kowalewski M, Bodnar RJ, Xiao S. 2012. Thermally-induced structural and chemical alteration of organic-walled microfossils: an experimental approach to understanding fossil preservation in metasediments. Geobiology. 10(5): 402–423.

Schopf JW, Ford TD, Breed WJ. 1973. Microorganisms from the late Precambrian of the Grand canyon, Arizona. Science. 179(4080): 1319–1321.

Schopf JW, Kitajima K, Spicuzza MJ, Kudryavtsev AB, Valley JW. 2018. SIMS analyses of the oldest known assemblage of microfossils document their taxon-correlated carbon isotope compositions. Proc Natl Acad Sci U S A. 115(1):53–58.

Schopf JW, Kudryavtsev AB, Agresti DG, Czaja AD, Wdowiak TJ. 2005. Raman imagery: a new approach to assess the geochemical maturity and biogenicity of permineralized Precambrian fossils. Astrobiology. 5(3):333–371.

Schopf JW, Kudryavtsev AB, Czaja AD, Tripathi AB. 2007. Evidence of Archean life: stromatolites and microfossils. Precambrian Res. 158(3–4):141–155.

Schopf JW, Kudryavtsev AB, Walter MR, Van Kranendonk MJ, Williford KH, Kozdon R, Valley JW, Gallardo VA, Espinoza C, Flannery DT. 2015. Sulfur-cycling fossil bacteria from the 1.8-Ga Duck Creek Formation provide promising evidence of evolution's null hypothesis. Proc Natl Acad Sci USA. 112(7):2087–2092.

Schopf JW, Sovietov YK. 1976. Microfossils in *Conophyton* from the Soviet Union and their bearing on Precambrian biostratigraphy. Science. 193(4248):143–146.

Schopf JW, Wei-Qing Z, Zhao-Liang X, Jen H. 1984. Proterozoic stromatolitic microbiotas of the 1400-1500 Ma-old Gaoyuzhuang formation near Jixian, northern China . Precambrian Res. 24:335–349.

Schopf JW. 1968. Microflora of the Bitter Springs formation, late Precambrian, central Australia. J Paleontol. 42:651–688.

Schopf JW. 1992. Proterozoic prokaryotes: affinities, geologic distribution, and evolutionary trends. In: Schopf JW, Klein C, editors. The Proterozoic Biosphere: A Multidisciplinary Study. Cambridge (UK): Cambridge University Press, p195–218.

Schopf JW. 2011. The paleobiological record of photosynthesis. Photosynth Res. 107:87–101.

Sergeev VN, Sharma M, Shukla Y. 2012. Proterozoic fossil cyanobacteria. Palaeobotanist. 61:189–358.

Strauss HD, Marais DJ, Hayes JM, Lambert IB, Summons RE. 1992a. Procedures of whole rock and kerogen analysis. In: Schopf JW, Klein C, editors. The Proterozoic Biosphere: A Multidisciplinary Study. Cambridge (UK): Cambridge University Press, p699–707.

Strauss H, Des Marais DJ, Summons RE, Hayes JM. 1992b. The carbon isotopic record. In: Schopf JW, Klein C, editors. The Proterozoic Biosphere: A Multidisciplinary Study. Cambridge (UK): Cambridge University Press, p117–128.

Strauss H, Moore TB. 1992. Abundances and isotopic compositions of carbon and sulfur species in whole rock and kerogen samples. In: Schopf JW, Klein C, editors. The Proterozoic Biosphere: A Multidisciplinary Study. Cambridge (UK): Cambridge University Press, p709–798.

Summons RE, Brassell SC, Eglinton G, Evans E, Horodyski RJ, Robinson N, Ward DM. 1988. Distinctive hydrocarbon biomarkers from fossiliferous sediment of the Late Proterozoic Walcott Member, Chuar Group, Grand Canyon, Arizona. Geochim Cosmochim Acta. 52(11):2625–2637.

Swett K, Knoll AH. 1989. Marine pisolites from upper Proterozoic carbonates of East Greenland and Spitsbergen. Sedimentology. 36(1): 75–93.

Tice MM, Bostick BC, Lowe DR. 2004. Thermal history of the 3.5–3.2 Ga Onverwacht and Fig Tree Groups, Barberton greenstone belt, South Africa, inferred by Raman microspectroscopy of carbonaceous material. Geol. 32(1):37–40.

Ueno Y, Isozaki Y, Yurimoto H, Maruyama S. 2001. Carbon isotopic signatures of individual Archean microfossils(?) from Western Australia. Int Geol Rev. 43(3):196–212.

Walsh MM, Lowe DR. 1985. Filamentous microfossils from the 3,500-Myr-old Onverwacht Group, Barberton Mountain Land, South Africa. Nature. 314(6011):530–532.

Walter MR, Hofmann HJ, Schopf JW. 1983. Geographic and geologic data for processed rock samples. In: Schopf JW, editor. Earth's Earliest Biosphere, its Origin and Evolution. Hoboken (NJ): Princeton University Press, p392.

Williford KH, Ushikubo T, Schopf JW, Lepot K, Kitajima K, Valley JW. 2013. Preservation and detection of microstructural and taxonomic correlations in the carbon isotopic compositions of individual Precambrian microfossils. Geochim Cosmochim Acta. 104:165–182.

Zerkle AL, House CH, Brantley SL. 2005. Biogeochemical signatures through time as inferred from whole microbial genomes. Am J Sci. 305(6–8):467–502.

Zhang Y. 1981. Proterozoic stromatolite microfloras of the Gaoyuzhuang Formation (Early Sinian: Riphean), Hebei, China. J Paleontol. 55:485–506.